JACS Au
AN OPEN ACCESS JOURNAL OF THE AMERICAN CHEMICAL SOCIETY
pubs.acs.org/jacsau
Letter

Nature of the Ultrafast Interligands Electron Transfers in Dye-Sensitized Solar Cells

Fulvio Perrella, Xiaosong Li, Alessio Petrone,* and Nadia Rega*

Cite This: *JACS Au* 2023, 3, 70−79
Read Online

ACCESS | Metrics & More | Article Recommendations | Supporting Information

ABSTRACT: Charge-transfer dynamics and interligand electron transfer (ILET) phenomena play a pivotal role in dye-sensitizers, mostly represented by the Ru-based polypyridyl complexes, for TiO_2 and ZnO-based solar cells. Starting from metal-to-ligand charge-transfer (MLCT) excited states, charge dynamics and ILET can influence the overall device efficiency. In this letter, we focus on $N3^{4-}$ dye ($[Ru(dcbpy)_2(NCS)_2]^{4-}$, dcbpy = 4,4′-dicarboxy-2,2′-bipyridine) to provide a first direct observation with high time resolution (<20 fs) of the ultrafast electron exchange between bpy-like ligands. ILET is observed in water solution after photo-excitation in the ~400 nm MLCT band, and assessment of its ultrafast time-scale is here given through a real-time electronic dynamics simulation on the basis of state-of-the-art electronic structure methods. Indirect effects of water at finite temperature are also disentangled by investigating the system in a symmetric gas-phase structure. As main result, remarkably, the ILET mechanism appears to be based upon a purely electronic evolution among the dense, experimentally accessible, MLCT excited states manifold at ~400 nm, which rules out nuclear−electronic couplings and proves further the importance of the dense electronic manifold in improving the efficiency of dye sensitizers in solar cell devices.

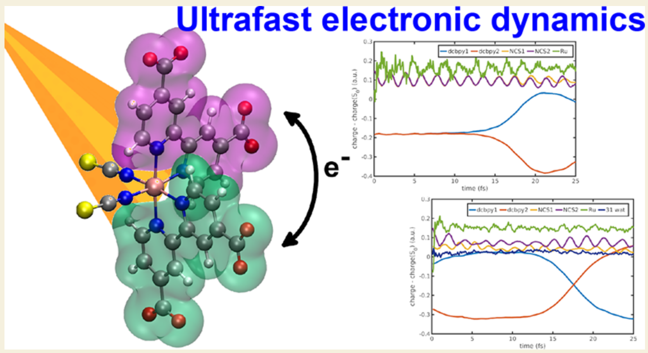

KEYWORDS: *Ru-polypyridyl complexes, dye sensitizers, interligand electron transfer, electronic dynamics, real-time time-dependent density functional theory*

Charge-transfer excited states, and in particular metal-to-ligand charge-transfer (MLCT), are essential for photo-excited energy transfer steps in many natural and artificial light-harvesting processes and photocatalysis.[1−6] Charge-transfer dynamics and interligand electron transfer (ILET) phenomena play a pivotal role in these emerging technologies and applications. ILET can potentially lead to a random mixture of charge-localized MLCT states, independent of which ligand the initial excitation localized the charge. This can influence the rate and the fate of the subsequent injection step in the substrate materials used in solar cell applications and, thus, the overall light-harvesting performances. For these reasons, the investigation of the charge injection mechanisms for dye−semiconductors has been the focus of several studies, with a particular attention on the related injection rates.[7−12] Among the most studied and employed nanostructured systems in this field are the dye sensitizers for TiO_2 and ZnO-based substrates for solar cells, mostly represented by the Ru-based polypyridyl complexes. In this regard, $[Ru(dcbpy)_2(NCS)_2]^{4-}$, dcbpy = (4,4′-dicarboxy-2,2′-bipyridine), or "$N3^{4-}$" (please see Figure S1 in the Supporting Information for $N3^{4-}$ molecular structure), belongs to a broad class of transition-metal compounds undergoing rapid and complex charge-transfer dynamics, potentially correlated with both a structural rearrangement and the polar environment (the solvent).[2,13−25] Electron−nuclear couplings and the electronic structure at the dye−substrate interface are believed to play key roles in determining the device function.[26−32] An additional layer of complexity is added because the general consensus is that N3 and its charged variants are characterized by complex dynamics that can involve multiple electronic states from the singlet initial ^{1}MLCT photoinduced state(s) in the visible range to the long-lived final triplet ^{3}MLCT, both in solution[33−38] and on semiconductor substrates.[1,39−45] Time-resolved studies in the infrared and terahertz regimes have identified remarkable differences between the dynamic response of dye−ZnO and dye−TiO_2 interfaces.[26,28−32,46−48] However, a complete understanding of the role (or not) of nuclear−electronic couplings in the early stage of MLCT before injection is difficult to achieve since the ultrafast ILET charge dynamics (<100 fs, where nuclear vibrations are not involved yet in a predominant way) cannot be directly observed because of the still limited time

Received: October 8, 2022
Revised: November 22, 2022
Accepted: November 23, 2022
Published: December 15, 2022

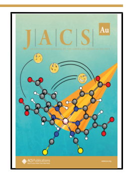

https://doi.org/10.1021/jacsau.2c00556
JACS Au 2023, 3, 70−79

resolution of experimental techniques.[7,26] Investigation of the occurrence or not of the ILET process in the ultrafast regime is the first step for disentangling (or not) the role in ILET of the nuclear vibrations from the ultrafast electronic dynamics of the dye sensitizer excited state electronic manifold. This is very important to understand, since ligands anchored on the substrate can be further stabilized by coordination with the Ti/Zn atoms of the substrates, which creates an even larger driving force for ILET to the proximal ligand and, thus, decreases the ILET barrier.

Time-dependent electronic structure theories can model the evolution in time of photoinduced excited electronic states from first principles. The wide adoption of density functional theory (DFT) and its time-dependent (TD) formulation has opened the doors in the recent years, indeed, to the *ab initio* characterization of both ground and excited-state properties for large macromolecular systems, such as those of biological[49−57] and materials[58−70] interest and their transient behavior.[71−73] DFT and TDDFT have shown to be effective for the theoretical characterization of many Ru complexes in different environments[74−98] and the vibrational dynamics of transient species.[99−104] Among nonperturbative approaches to mean-field quantum electronic dynamics (ED), real-time time-dependent density functional theory (RT-TDDFT) has been proven to be very powerful and provides a molecular interpretation of the interplay between initial photoexcited states and exciton and polaron formation,[102,105−108] also including relativistic effects.[109,110] In this letter, we present the ultrafast hole−electron dynamics of two experimentally relevant $N3^{4-}$ photoinduced charge-transfer excited states (belonging to the 372 nm band[111]), where the system is characterized and propagated both in water solution and in gas-phase, which demonstrates the crucial role of the dense electronic manifold of metal complexes for the initial ultrafast ILET, even before the nuclear-electron couplings have a substantial impact on the CT dynamics.[112] Such states, called $^1MLCT_A$ and $^1MLCT_B$ and respectively found around 24 400−24 700 cm^{-1} (410−405 nm) and 25 000−25 300 cm^{-1} (400−395 nm), were previously shown to be those most vibronically coupled with the final triplet one.[111] Both states are characterized by an important electronic density redistribution from the $Ru(NCS)_2$ moiety toward the dcbpy rings, with a transition electric dipole moment predominantly located on the $N3^{4-}$ equatorial plane.[111]

Effects by solvation and structural distortions from the symmetric, minimum energy structure (due to finite temperature and the environment) on photoinduced MLCT states and subsequent ultrafast charge rearrangements were considered. No explicit effects of temperature were included in the electronic degrees of freedom. In this work, we are not limited to the vertical excitation picture from the minimum of the ground state, and the distortions due to the environment and thermal fluctuations are indeed included, although in an average manner, by employing a representative configuration, given also the high computational cost related to RT-TDDFT simulations. The excited electronic density was, in fact, propagated via RT-TDDFT on a representative configuration extracted from a previously collected *ab initio* molecular dynamics (AIMD) trajectory in water solution, hereafter referred to as D-W structure (see Figure S7 in the Supporting Information). Additionally for interested readers, please refer to Section 5 and to Section 2 in the Supporting Information, along with ref 113, for RT-TDDFT electronic dynamics and AIMD computational details, respectively. The chosen configuration features relevant Ru(II) coordination structural parameters (Figure S3), overall symmetry distortion in water from an ideally C_2 configuration (Figure S5), as well as ligands' solvation with a proper number of explicit solvent molecules (Figure 1 and Figure S4) that are representative of room

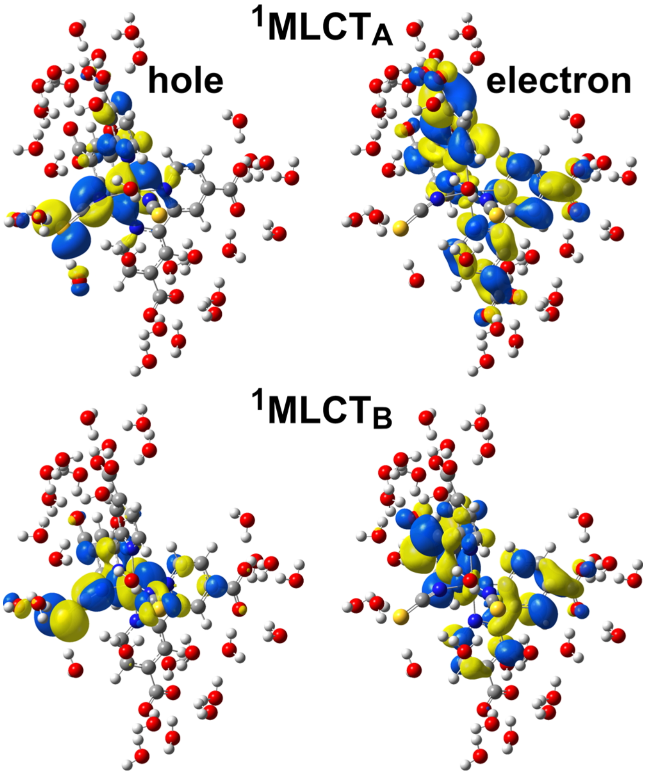

Figure 1. $^1MLCT_A$ and $^1MLCT_B$ excited states characterized by NTOs (D-W structure). Hole and electron isodensity plots (0.02 isovalue) are reported on left and right panels, respectively. NTOs are calculated to provide a simpler orbital interpretation of electronic excitations, which results in a hole−electron pair of orbitals.[114]

temperature structural equilibrium, controlling also the NCS ligands' coordination, given their lability in solution, as witnessed by inspecting AIMD structural distributions (please refer to Section 2 and Figures S3−S5 of the Supporting Information and ref 113).

We first analyzed the nature of the excited states by linear-response (LR-) TD-DFT calculations (please refer to Table S1 in the Supporting Information). Two main effects of the symmetry lowering in aqueous solution were observed on the nature of the photogenerated MLCT states: (i) excited states were more accessible compared with the ones that appear dark in the C_2 gas-phase optimized arrangement (hereafter called M-G structure) and (ii) the photoexcited electrons in MLCT states were now more localized. In fact, the $^1MLCT_A$ state appeared brighter in the vibrationally distorted, water-solvated, D-W structure, whereas it was dark in the M-G symmetric arrangement, representative of the gas phase. The photoelectron localization could be gauged by inspecting a direct spatial representation of the hole−electron charge redistribution by Natural Transition Orbital analysis[114] [NTOs, reported in Figure 1 for $^1MLCT_A$ (upper panels) and $^1MLCT_B$ (lower panels)]. In both CT excitations, electron density is always removed from a combination of NCS^- π^* and

https://doi.org/10.1021/jacsau.2c00556
JACS Au 2023, 3, 70−79

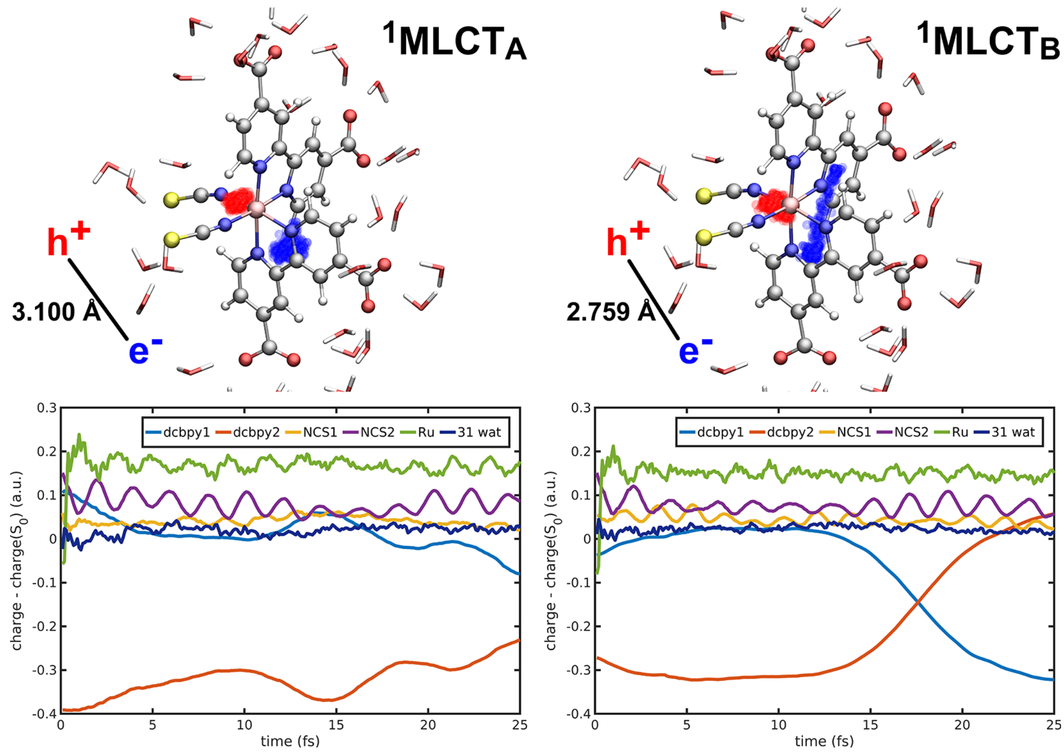

Figure 2. Electronic dynamics of ^{1}MLCT$_A$ (left) and ^{1}MLCT$_B$ (right) states for D-W N3^{4-} structure in water solution. Top: hole (in red) and electron (in blue) barycenter spatial distributions. Hole/electron RMS distances are also reported in the figure. Bottom: time-dependent fragment charges (with respect to the S$_0$ state). Hole and electron RMS velocities are 0.777 and 0.766 Å fs^{-1} for ^{1}MLCT$_A$ state and 0.838 and 0.760 Å fs^{-1} for ^{1}MLCT$_B$ state, respectively.

Ru d orbitals to relocate on the whole dcbpy ligands (^{1}MLCT$_A$) or more on the dcbpy aromatic rings (the dcbpy portions labeled with 1b or 2b in Figure S1) in a *trans* orientation with respect to the NCS$^-$ ligands (^{1}MLCT$_B$).

Then, the ultrafast CT electronic dynamics through RT-TDDFT were analyzed. The electronic densities to be propagated, resembling an electronic excitation, were prepared according to a well-established procedure.[71,107,108,115−117] In brief, the orbitals' population is adjusted by promoting an electron from a selected occupied molecular orbital to another one that is unoccupied in the ground state ("Koopman excitation"). Koopman excitation is a very easy procedure for preparing an initial state resembling an electronic excitation via a nonstationary superposition of excited states.[118] Although specific and experimentally tailored approaches have been also proposed over the years for mimicking excitations,[119−121] the procedure used in this work is very effective given the size of the system and the resulting affordable computational cost. Electromagnetic radiation instantaneously induces exciton formation in N3^{4-}; therefore, the subsequent hole−electron dynamics can be analyzed as time-dependent charge differences with respect to the equilibrium ground state, S$_0$. In particular, we report in Figure 2 the evolution in time of the charge differences localized on dcbpy1 and 2, NCS1 and 2, and Ru molecular fragments, together with spatial distributions of the positive and negative charge differences since they provide an immediate view of the hole−electron formation and dynamics. The hole and electron positions can be taken as the barycenters of the positive and negative atomic charges, respectively.

Concerning ^{1}MLCT$_A$ excitation, the hole barycenter is located between NCS2 and Ru, while the electron one is found nearly between dcbpy2 rings (Figure 2, top left panel). Regarding the time evolution of the electronic density, we can observe the charge migration from the NCS2 and dcbpy1 ligands onto both dcbpy2 rings (Figure 2, bottom left panel). The charge carriers appear quite separated and show a 3.100 Å average distance. Their mobility is moreover comparable (0.777 and 0.766 Å fs^{-1} hole and electron average velocities, respectively). While NCS1 density is almost constant along the simulation, the hole is shared between NCS2 and Ru center at a fast 16 012 cm^{-1} exchange frequency. Nevertheless, the hole appears more localized on the Ru center and not equally shared. After the ^{1}MLCT$_A$ photoexcitation, the electron appears instead to be moderately stable on the dcbpy2 ligand, because no major charge transfer between the two dcbpy ligands is observed.

Similarly to ^{1}MLCT$_A$, we observe that the initial ^{1}MLCT$_B$ excitation (t = 0) asymmetrically places the photoexcited electron from NCS2 and NCS1 mainly onto one dcbpy ligand (dcbpy2) (Figure 2, bottom right panel). The hole barycenter, again located near the (NCS)$_2$Ru moiety, now is more symmetrically found between the two NCS$^-$ ligands (Figure 2, top right panel). On the contrary, the electron barycenter explores a wider region, moving from dcbpy2 in the first part of the trajectory (near the dcbpy2a axial ring), toward the dcbpy1b equatorial ring on the other acceptor ligand (after ~15 fs). Similar hole/electron RMS distance (2.759 Å), hole (0.838 Å fs^{-1}), and electron (0.760 Å fs^{-1}) RMS velocities are found. The hole is shared between NCS2 and Ru(II) at 16 012 and 20 015 cm^{-1} frequencies, in a less clear way than in ^{1}MLCT$_A$ (Figure 2, bottom right panel). Again, the hole is more concentrated on the Ru center. In contrast to ^{1}MLCT$_A$, the ^{1}MLCT$_B$ photoinduced electron is hosted by dcbpy2 for

https://doi.org/10.1021/jacsau.2c00556
JACS Au 2023, 3, 70−79

~15 fs and then completely transferred to dcbpy1 within the simulated 25 fs time. An ultrafast ILET process based upon an intrinsic electronic dynamics is therefore observed for the $^1MLCT_B$ $N3^{4-}$ state in water solution at finite temperature.

Electron−nuclear couplings and effects of environmental phonons can potentially induce charge localization during the charge dynamics. Such relaxation processes based upon internal conversion and intersystem crossing, which occur on ~50−100 fs time scales, have been previously investigated both from an experimental and computational point of view.[33,122−124] On ultrafast time scales, nuclei can instead be considered fixed, and from the results in this letter, it appears that pure electron couplings within electronic states are responsible for the observed ultrafast ILET in solution, which causes charge randomization on the acceptors on a time scale faster than nuclear motions, thereby potentially already promoting subsequent ultrafast charge injection into the substrate. Excited states characterization and electronic dynamics were also performed on the gas-phase, symmetric, and optimized M-G structure, excluding any structural distortion and solvation effects, to rule out the indirect effects induced by dynamics in water at finite temperature and to further assess the purely electronic nature of ILET processes in transition metal compounds like $N3^{4-}$. As expected, the structural C_2 symmetry is reflected in $^1MLCT_A$ and $^1MLCT_B$ NTOs spatial distributions. In particular, the photoexcited electron is symmetrically distributed between the two acceptor ligands (Figure 3), placed on both axial and equatorial rings ($^1MLCT_A$) or only on the equatorial rings, *trans* to the NCS^- ligands ($^1MLCT_B$). The hole is symmetrically found on both the NCS^- ligands, as well.

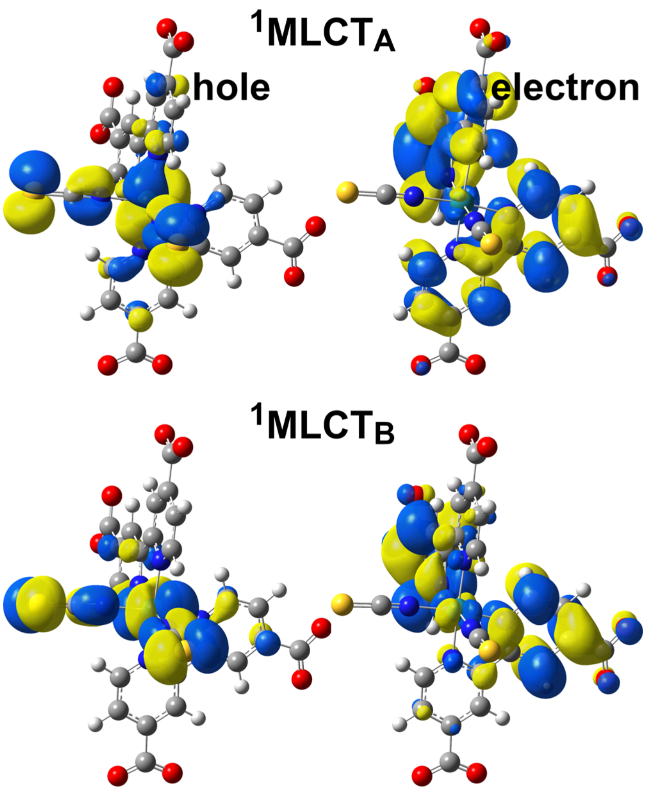

Figure 3. $^1MLCT_A$ and $^1MLCT_B$ excited states characterized by NTOs (M-G structure). Hole and electron isodensity plots (0.02 isovalue) are reported on left and right panels, respectively.

As matter of fact, the $t = 0$ initial states of both electronic dynamics are, thus, symmetric (no indirect effects on photoinduced hole−electron density induced by the environment). In $^1MLCT_A$ state propagation, the hole and the electron barycenters oscillate along the C_2 symmetry axis (Figure 4, top left panel) but with different mobility (1.223 and 0.684 Å fs^{-1} RMS velocities, respectively). In particular, the photoexcited electron remains symmetrically spread between the two acceptor dcbpy ligands along all the simulation (Figure 4, bottom left panel). As previously observed in water, an ultrafast ILET process is triggered by the $^1MLCT_B$ equatorial excitation, although in this case it cannot by ascribed to distortions induced by the finite temperature and solvation because of the highly symmetric structure. In particular, the $^1MLCT_B$ electronic dynamics on the symmetric M-G structure features a lowering of the symmetry of the initial photoexcited electron spatial distribution, starting from ~15 fs (Figure 4, bottom right panel), whose barycenter deviates from the symmetry axis (Figure 4, top right panel). The electron mobility appears moreover increased (0.939 Å fs^{-1}). Several movies of CT dynamics are provided as additional Supporting Files to better display the hole−electron $^1MLCT_A$ and $^1MLCT_B$ dynamics on $N3^{4-}$ D-W and M-G structures.

RT-TDDFT electronic dynamics simulations are used as a mean-field approach to study ultrafast photoinduced charge dynamics and are capable of capturing randomization of the charge transfer on the acceptor ligands. Thus, in this letter, we clearly observe an ILET process on an ultrafast time-scale that is within 15 fs. The intricate electronic manifold can, indeed, induce a randomization of the initial localized excitation via ILET. This process occurs faster than vibrations can start to play an important role, and thus, the charge injection into the substrate can happen before that nuclear motions can further localize the excitations. This was possible by analyzing the RT-TDDFT electronic dynamics simulations, which are capable of disentangling electronic and nuclear effects on such short (not easily experimentally accessible) time scales. Previous experimental works already suggested that ILET processes can occur in the Franck−Condon region or in the ^1MLCT excited state(s), i.e., before the intersystem crossing toward the ^3MLCT state, for the extensively studied $Ru(bpy)_3^{2+}$,[20,125−131] as well as for $N3^{4-}$.[26] However, an ultrafast time-scale of ILET could be only indirectly inferred from experimental measurements, which in fact can only actually probe the final triplet state. This work is, instead, the first direct observation of ultrafast electron exchange between bpy-like ligands in $N3^{4-}$ dye with such ultrafast time resolution. Remarkably, the ILET mechanism appears to be based upon a purely electronic evolution among the dense, experimentally accessible, MLCT excited state manifold at ~400 nm, which rules out nuclear−electronic couplings. Specific CT excitations (such as $^1MLCT_B$ state) seem to actually promote ILET at ~15 fs after the photoexcitation. As a practical consequence, our study predicts that ILET does not necessarily require nuclear motions to occur and cannot be a rate-limiting step for following electron injection into the semiconductor substrate. The deep comprehension of the dynamic behavior of the MLCT states and the dense electronic manifold is relevant for photoharvesting and can be useful to improve the efficiency of dye sensitizers in solar cell devices. We believe that this work will motivate other groups to utilize RT-TDDFT simulations for testing and designing better performing dye sensitizers to

https://doi.org/10.1021/jacsau.2c00556
JACS Au 2023, 3, 70−79

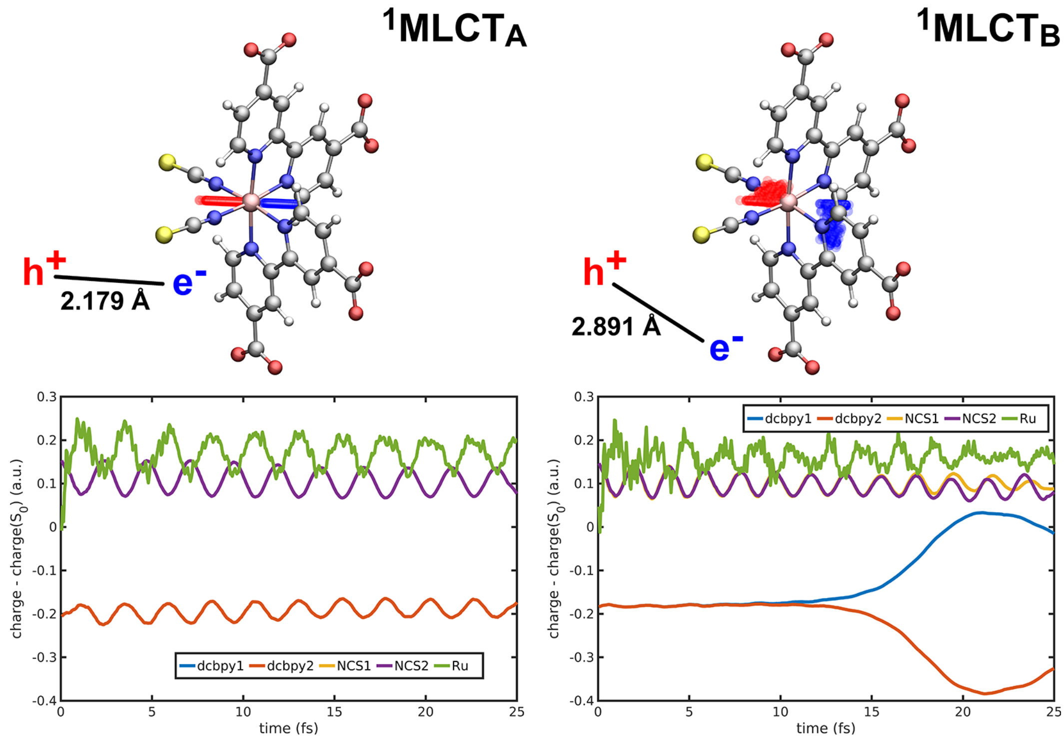

Figure 4. Electronic dynamics of ^{1}MLCT$_A$ (left) and ^{1}MLCT$_B$ (right) states for M-G symmetric, gas-phase $N3^{4-}$ structure. Top: hole (in red) and electron (in blue) barycenter spatial distributions. Hole/electron RMS distances are also reported in the figure. Bottom: time-dependent fragments' charges (with respect to the S_0 state). Hole and electron RMS velocities are 1.223 and 0.684 Å fs^{-1} for the ^{1}MLCT$_A$ state and 1.190 and 0.939 Å fs^{-1} for the ^{1}MLCT$_B$ state, respectively. Note that for the ^{1}MLCT$_A$ state, the dcbpy1 and dcbpy2 time-dependent charges are equal along the entire simulation and, thus, are completely superimposed.

exploit the role of symmetry, electronic nature of ligands, and the nature of the environment in the ultrafast charge dynamics that rule the charge injection into substrates.

METHODS

LR- and RT-TDDFT calculations were performed using a development version of the Gaussian suite of programs.[132] $N3^{4-}$ electronic structures were obtained by solving the Kohn–Sham equations employing the B3LYP exchange–correlation functional[133−135] with the def2-SVP[136] basis set and corresponding electronic core potential (ECP) for Ru.[137] Such level of theory was already validated in previous studies about $N3^{4-}$ S_0 and T states structural characterization in solution, electronic, and X-ray transitions.[68,79,113,138]

All the electronic dynamics trajectories were simulated for 25 fs. The modified midpoint unitary transformation (MMUT) method was employed to propagate the RT-TDDFT equations.[139] Please refer to Section 5 in the Supporting Information for details about the integration procedure and the main text for the preparation of the initial density reproducing the excitation. A time step of 1 as ($N3^{4-}$ M-G structure) or 2 as (D-W structure) was chosen, which allowed an energy conservation within 10^{-6} hartree.

ASSOCIATED CONTENT

Supporting Information

The following files are available free of charge: The Supporting Information is available free of charge at https://pubs.acs.org/doi/10.1021/jacsau.2c00556.

$N3^{4-}$ structure and fragments partition, $N3^{4-}$ *ab initio* molecular dynamics in explicit water solution, $N3^{4-}$ structure for electronic dynamics, $N3^{4-}$ excited states, and real-time time-dependent density functional theory (PDF)

rt_hole_el_dw_a.mpg: movie of hole–electron barycenters dynamics, A state, D-W structure (MPG)

rt_hole_el_dw_b.mpg: movie of hole–electron barycenters dynamics, B state, D-W structure (MPG)

rt_hole_el_mg_a.mpg: movie of hole–electron barycenters dynamics, A state, M-G structure (MPG)

rt_hole_el_mg_b.mpg: movie of hole–electron barycenters dynamics, B state, M-G structure (MPG)

AUTHOR INFORMATION

Corresponding Authors

Alessio Petrone − *Department of Chemical Sciences, University of Napoli Federico II, I-80126 Napoli, Italy; Scuola Superiore Meridionale, I-80138 Napoli, Italy; Istituto Nazionale Di Fisica Nucleare, sezione di Napoli, 80126 Napoli, Italy;* orcid.org/0000-0003-2232-9934; Email: alessio.petrone@unina.it

Nadia Rega − *Department of Chemical Sciences, University of Napoli Federico II, I-80126 Napoli, Italy; Scuola Superiore Meridionale, I-80138 Napoli, Italy; Istituto Nazionale Di Fisica Nucleare, sezione di Napoli, 80126 Napoli, Italy; CRIB, Centro Interdipartimentale di Ricerca sui Biomateriali, I-80125 Napoli, Italy;* orcid.org/0000-0002-2983-766X; Email: nadia.rega@unina.it

Authors

Fulvio Perrella − *Department of Chemical Sciences, University of Napoli Federico II, I-80126 Napoli, Italy;* Present

Address: Scuola Superiore Meridionale, Largo San Marcellino 10, I-80138 Napoli, Italy; orcid.org/0000-0003-3376-5897

Xiaosong Li − *Department of Chemistry, University of Washington, Seattle, Washington 98195, United States*; orcid.org/0000-0001-7341-6240

Complete contact information is available at: https://pubs.acs.org/10.1021/jacsau.2c00556

Author Contributions

CRediT: **Fulvio Perrella** data curation, formal analysis, investigation, writing-original draft, writing-review & editing; **Xiaosong Li** methodology, software, writing-review & editing; **Alessio Petrone** conceptualization, methodology, software, supervision, validation, writing-original draft, writing-review & editing; **Nadia Rega** conceptualization, funding acquisition, methodology, supervision, writing-original draft, writing-review & editing.

Notes

The authors declare no competing financial interest.

ACKNOWLEDGMENTS

F.P. and N.R. thank Gaussian Inc. for financial support. The Italian Ministry of Education, University and Research (MIUR) is also gratefully acknowledged for financial support (A.P., Project AIM1829571-1 CUP E61G19000090002; N.R., Project PRIN 2017YJMPZN001, PRIN 202082CE3T_002). The development of the TDDFT method was supported by the US National Science Foundation (CHE-2154346 to X.L.). Computational L-edge spectroscopy applications were partially supported by the U.S. Department of Energy, Office of Science, Office of Basic Energy Sciences, Division of Chemical Sciences, Geosciences and Biosciences, through Argonne National Laboratory under Contract No. DE-AC02-06CH11357.

REFERENCES

(1) Anderson, N. A.; Lian, T. Ultrafst Electron Transfer at the Molecule-Semiconductor Nanoparticle Interface. *Annu. Rev. Phys. Chem.* **2005**, *56*, 491−519.

(2) Grätzel, M. Solar Energy Conversion by Dye-Sensitized Photovoltaic Cells. *Inorg. Chem.* **2005**, *44*, 6841−6851.

(3) Ardo, S.; Meyer, G. J. Photodriven Heterogeneous Charge Transfer with Transition-Metal Compounds Anchored to TiO_2 Semiconductor Surfaces. *Chem. Soc. Rev.* **2009**, *38*, 115−164.

(4) Hagfeldt, A.; Boschloo, G.; Sun, L.; Kloo, L.; Pettersson, H. Dye-Sensitized Solar Cells. *Chem. Rev.* **2010**, *110*, 6595−6663.

(5) Mirkovic, T.; Ostroumov, E. E.; Anna, J. M.; van Grondelle, R.; Govindjee; Scholes, G. D. Light Absorption and Energy Transfer in the Antenna Complexes of Photosynthetic Organisms. *Chem. Rev.* **2017**, *117*, 249−293.

(6) Hagfeldt, A.; Grätzel, M. Molecular Photovoltaics. *Acc. Chem. Res.* **2000**, *33*, 269−277.

(7) Siefermann, K. R.; Pemmaraju, C. D.; Neppl, S.; Shavorskiy, A.; Cordones, A. A.; Vura-Weis, J.; Slaughter, D. S.; Sturm, F. P.; Weise, F.; Bluhm, H.; Strader, M. L.; Cho, H.; Lin, M.-F.; Bacellar, C.; Khurmi, C.; Guo, J.; Coslovich, G.; Robinson, J. S.; Kaindl, R. A.; Schoenlein, R. W.; Belkacem, A.; Neumark, D. M.; Leone, S. R.; Nordlund, D.; Ogasawara, H.; Krupin, O.; Turner, J. J.; Schlotter, W. F.; Holmes, M. R.; Messerschmidt, M.; Minitti, M. P.; Gul, S.; Zhang, J. Z.; Huse, N.; Prendergast, D.; Gessner, O. Atomic-Scale Perspective of Ultrafast Charge Transfer at a Dye−Semiconductor Interface. *J. Phys. Chem. Lett.* **2014**, *5*, 2753−2759.

(8) Chergui, M.; Collet, E. Photoinduced Structural Dynamics of Molecular Systems Mapped by Time-Resolved X-ray Methods. *Chem. Rev.* **2017**, *117*, 11025−11065.

(9) Baldini, E.; Palmieri, T.; Rossi, T.; Oppermann, M.; Pomarico, E.; Auböck, G.; Chergui, M. Interfacial Electron Injection Probed by a Substrate-Specific Excitonic Signature. *J. Am. Chem. Soc.* **2017**, *139*, 11584−11589.

(10) Govind Rao, V.; Lu, H. P. Inhomogeneous and Complex Interfacial Electron-Transfer Dynamics: A Single-Molecule Perspective. *ACS Energy Lett.* **2016**, *1*, 773−791.

(11) Wei, H.; Luo, J.-W.; Li, S.-S.; Wang, L.-W. Revealing the Origin of Fast Electron Transfer in TiO_2-Based Dye-Sensitized Solar Cells. *J. Am. Chem. Soc.* **2016**, *138*, 8165−8174.

(12) Frontiera, R. R.; Dasgupta, J.; Mathies, R. A. Probing Interfacial Electron Transfer in Coumarin 343 Sensitized TiO_2 Nanoparticles with Femtosecond Stimulated Raman. *J. Am. Chem. Soc.* **2009**, *131*, 15630−15632.

(13) Damrauer, N. H.; Cerullo, G.; Yeh, A.; Boussie, T. R.; Shank, C. V.; McCusker, J. K. Femtosecond Dynamics of Excited-State Evolution in $[Ru(bpy)_3]^{2+}$. *Science* **1997**, *275*, 54−57.

(14) McCusker, J. K.; Vlček, A. Ultrafast Excited-State Processes in Inorganic Systems. *Acc. Chem. Res.* **2015**, *48*, 1207−1208. (Special Issue and references therein).

(15) Hagfeldt, A.; Boschloo, G.; Sun, L.; Kloo, L.; Pettersson, H. Dye-sensitized solar cells. *Chem. Rev.* **2010**, *110*, 6595−6663.

(16) Chung, I.; Lee, B.; He, J.; Chang, R. P. H.; Kanatzidis, M. G. All-solid-state dye-sensitized solar cells with high efficiency. *Nature* **2012**, *485*, 486−489.

(17) Grätzel, M. Dye-sensitized solar cells. *J. Photoch. Photobio. C* **2003**, *4*, 145−153.

(18) Chergui, M. Ultrafast Photophysics of Transition Metal Complexes. *Acc. Chem. Res.* **2015**, *48*, 801−808.

(19) Juban, E. A.; Smeigh, A. L.; Monat, J. E.; McCusker, J. K. Ultrafast dynamics of ligand-field excited states. *Coordin. Chem. Rev.* **2006**, *250*, 1783−1791.

(20) McCusker, J. K. Femtosecond absorption spectroscopy of transition metal charge-transfer complexes. *Acc. Chem. Res.* **2003**, *36*, 876−887.

(21) Nazeeruddin, M. K.; Humphry-Baker, R.; Liska, P.; Grätzel, M. Investigation of sensitizer adsorption and the influence of protons on current and voltage of a dye-sensitized nanocrystalline TiO_2 solar cell. *J. Phys. Chem. B* **2003**, *107*, 8981−8987.

(22) Meng, Q.-B.; Takahashi, K.; Zhang, X.-T.; Sutanto, I.; Rao, T.; Sato, O.; Fujishima, A.; Watanabe, H.; Nakamori, T.; Uragami, M. Fabrication of an efficient solid-state dye-sensitized solar cell. *Langmuir* **2003**, *19*, 3572−3574.

(23) Plasser, F.; Barbatti, M.; Aquino, A. J.; Lischka, H. Electronically excited states and photodynamics: a continuing challenge. *Theor. Chem. Acc.* **2012**, *131*, 1073.

(24) Tavernelli, I.; Curchod, B. F.; Rothlisberger, U. Nonadiabatic molecular dynamics with solvent effects: A LR-TDDFT QM/MM study of ruthenium (II) tris (bipyridine) in water. *Chem. Phys.* **2011**, *391*, 101−109. Open problems and new solutions in time-dependent density functional theory.

(25) Hart, S. M.; Silva, W. R.; Frontiera, R. R. Femtosecond stimulated Raman evidence for charge-transfer character in pentacene singlet fission. *Chem. Sci.* **2018**, *9*, 1242−1250.

(26) Rimgard, B. P.; Föhlinger, J.; Petersson, J.; Lundberg, M.; Zietz, B.; Woys, A. M.; Miller, S. A.; Wasielewski, M. R.; Hammarström, L. Ultrafast interligand electron transfer in cis-$[Ru(4,4'\text{-dicarboxylate-}2,2'\text{-bipyridine})_2(NCS)_2]^{4-}$ and implications for electron injection limitations in dye sensitized solar cells. *Chem. Sci.* **2018**, *9*, 7958−7967.

(27) Anta, J. A.; Guillén, E.; Tena-Zaera, R. ZnO-Based Dye-Sensitized Solar Cells. *J. Phys. Chem. C* **2012**, *116*, 11413−11425.

(28) Tiwana, P.; Docampo, P.; Johnston, M. B.; Snaith, H. J.; Herz, L. M. Electron Mobility and Injection Dynamics in Mesoporous ZnO, SnO_2, and TiO_2 Films Used in Dye-Sensitized Solar Cells. *ACS Nano* **2011**, *5*, 5158−5166.

(29) Katoh, R.; Furube, A.; Yoshihara, T.; Hara, K.; Fujihashi, G.; Takano, S.; Murata, S.; Arakawa, H.; Tachiya, M. Efficiencies of Electron Injection from Excited N3 Dye into Nanocrystalline Semiconductor (ZrO_2, TiO_2, ZnO, Nb_2O_5, SnO_2, In_2O_3) Films. *J. Phys. Chem. B* **2004**, *108*, 4818−4822.
(30) Němec, H.; Rochford, J.; Taratula, O.; Galoppini, E.; Kužel, P.; Polívka, T.; Yartsev, A.; Sundström, V. Influence of the Electron-Cation Interaction on Electron Mobility in Dye-Sensitized ZnO and TiO_2 Nanocrystals: A Study Using Ultrafast Terahertz Spectroscopy. *Phys. Rev. Lett.* **2010**, *104*, 197401.
(31) Strothkämper, C.; Bartelt, A.; Sippel, P.; Hannappel, T.; Schütz, R.; Eichberger, R. Delayed Electron Transfer through Interface States in Hybrid ZnO/Organic-Dye Nanostructures. *J. Phys. Chem. C* **2013**, *117*, 17901−17908.
(32) Stockwell, D.; Yang, Y.; Huang, J.; Anfuso, C.; Huang, Z.; Lian, T. Comparison of Electron-Transfer Dynamics from Coumarin 343 to TiO_2, SnO_2, and ZnO Nanocrystalline Thin Films: Role of Interface-Bound Charge-Separated Pairs. *J. Phys. Chem. C* **2010**, *114*, 6560−6566.
(33) Asbury, J. B.; Ellingson, R. J.; Ghosh, H. N.; Ferrere, S.; Nozik, A. J.; Lian, T. Femtosecond IR Study of Excited-State Relaxation and Electron-Injection Dynamics of $Ru(dcbpy)_2(NCS)_2$ in Solution and on Nanocrystalline TiO_2 and Al_2O_3 Thin Films. *J. Phys. Chem. B* **1999**, *103*, 3110−3119.
(34) Waterland, M. R.; Kelley, D. F. Photophysics and Relaxation Dynamics of Ru(4,4′Dicarboxy-2,2′-bipyridine)$_2$cis(NCS)$_2$ in Solution. *J. Phys. Chem. A* **2001**, *105*, 4019−4028.
(35) Shoute, L. C. T.; Loppnow, G. R. Excited-State Metal-to-Ligand Charge Transfer Dynamics of a Ruthenium(II) Dye in Solution and Adsorbed on TiO_2 Nanoparticles from Resonance Raman Spectroscopy. *J. Am. Chem. Soc.* **2003**, *125*, 15636−15646.
(36) Van Kuiken, B. E.; Huse, N.; Cho, H.; Strader, M. L.; Lynch, M. S.; Schoenlein, R. W.; Khalil, M. Probing the Electronic Structure of a Photoexcited Solar Cell Dye with Transient X-ray Absorption Spectroscopy. *J. Phys. Chem. Lett.* **2012**, *3*, 1695−1700.
(37) Bräm, O.; Messina, F.; El-Zohry, A. M.; Cannizzo, A.; Chergui, M. Polychromatic Femtosecond Fluorescence Studies of Metal-Polypyridine Complexes in Solution. *Chem. Phys.* **2012**, *393*, 51−57.
(38) Horvath, R.; Fraser, M. G.; Clark, C. A.; Sun, X.-Z.; George, M. W.; Gordon, K. C. Nature of Excited States of Ruthenium-Based Solar Cell Dyes in Solution: A Comprehensive Spectroscopic Study. *Inorg. Chem.* **2015**, *54*, 11697−11708.
(39) Tachibana, Y.; Moser, J. E.; Grätzel, M.; Klug, D. R.; Durrant, J. R. Subpicosecond Interfacial Charge Separation in Dye-Sensitized Nanocrystalline Titanium Dioxide Films. *J. Phys. Chem.* **1996**, *100*, 20056−20062.
(40) Hannappel, T.; Burfeindt, B.; Storck, W.; Willig, F. Measurement of Ultrafast Photoinduced Electron Transfer from Chemically Anchored Ru-Dye Molecules into Empty Electronic States in a Colloidal Anatase TiO_2 Film. *J. Phys. Chem. B* **1997**, *101*, 6799−6802.
(41) Durrant, J. R.; Tachibana, Y.; Mercer, I.; Moser, J. E.; Grätzel, M.; Klug, D. R. The Excitation Wavelength and Solvent Dependance of the Kinetics of Electron Injection in $Ru(dcbpy)_2(NCS)_2$ Sensitized Nanocrystalline TiO_2 Films. *Z. Phys. Chem.* **1999**, *212*, 93−98.
(42) Asbury, J. B.; Hao, E.; Wang, Y.; Ghosh, H. N.; Lian, T. Ultrafast Electron Transfer Dynamics from Molecular Adsorbates to Semiconductor Nanocrystalline Thin Films. *J. Phys. Chem. B* **2001**, *105*, 4545−4557.
(43) Kallioinen, J.; Benkö, G.; Sundström, V.; Korppi-Tommola, J. E. I.; Yartsev, A. P. Electron Transfer from the Singlet and Triplet Excited States of $Ru(dcbpy)_2(NCS)_2$ into Nanocrystalline TiO_2 Thin Films. *J. Phys. Chem. B* **2002**, *106*, 4396−4404.
(44) Asbury, J. B.; Anderson, N. A.; Hao, E.; Ai, X.; Lian, T. Parameters Affecting Electron Injection Dynamics from Ruthenium Dyes to Titanium Dioxide Nanocrystalline Thin Film. *J. Phys. Chem. B* **2003**, *107*, 7376−7386.
(45) Rich, C. C.; Mattson, M. A.; Krummel, A. T. Direct Measurement of the Absolute Orientation of N3 Dye at Gold and Titanium Dioxide Surfaces with Heterodyne-Detected Vibrational SFG Spectroscopy. *J. Phys. Chem. C* **2016**, *120*, 6601−6611.
(46) Rehm, J. M.; McLendon, G. L.; Nagasawa, Y.; Yoshihara, K.; Moser, J.; Grätzel, M. Femtosecond Electron-Transfer Dynamics at a Sensitizing Dye-Semiconductor (TiO_2) Interface. *J. Phys. Chem.* **1996**, *100*, 9577−9578.
(47) Furube, A.; Katoh, R.; Hara, K.; Murata, S.; Arakawa, H.; Tachiya, M. Ultrafast Stepwise Electron Injection from Photoexcited Ru-Complex into Nanocrystalline ZnO Film via Intermediates at the Surface. *J. Phys. Chem. B* **2003**, *107*, 4162−4166.
(48) Anderson, N. A.; Lian, T. Ultrafast Electron Transfer at the Molecule-Semiconductor Nanoparticle Interface. *Annu. Rev. Phys. Chem.* **2005**, *56*, 491−519.
(49) Battista, E.; Scognamiglio, P. L.; Di Luise, N.; Raucci, U.; Donati, G.; Rega, N.; Netti, P. A.; Causa, F. Turn-on Fluorescence Detection of Protein by Molecularly Imprinted Hydrogels Based on Supramolecular Assembly of Peptide Multi-Functional Blocks. *J. Mater. Chem. B* **2018**, *6*, 1207−1215.
(50) Wildman, A.; Donati, G.; Lipparini, F.; Mennucci, B.; Li, X. Nonequilibrium Environment Dynamics in a Frequency-Dependent Polarizable Embedding Models. *J. Chem. Theory Comput.* **2019**, *15*, 43−51.
(51) Perrella, F.; Raucci, U.; Chiariello, M. G.; Chino, M.; Maglio, O.; Lombardi, A.; Rega, N. Unveiling the structure of a novel artificial heme-enzyme with peroxidase-like activity: A theoretical investigation. *Biopolymers* **2018**, *109*, No. e23225.
(52) Lever, G.; Cole, D. J.; Lonsdale, R.; Ranaghan, K. E.; Wales, D. J.; Mulholland, A. J.; Skylaris, C.-K.; Payne, M. C. Large-Scale Density Functional Theory Transition State Searching in Enzymes. *J. Phys. Chem. Lett.* **2014**, *5*, 3614−3619.
(53) Curutchet, C.; Mennucci, B. Quantum Chemical Studies of Light Harvesting. *Chem. Rev.* **2017**, *117*, 294−343.
(54) Donati, G.; Petrone, A.; Caruso, P.; Rega, N. The Mechanism of a Green Fluorescent Protein Proton Shuttle Unveiled in the Time-Resolved Frequency Domain by Excited State Ab Initio Dynamics. *Chem. Sci.* **2018**, *9*, 1126−1135.
(55) Raucci, U.; Perrella, F.; Donati, G.; Zoppi, M.; Petrone, A.; Rega, N. Ab-initio molecular dynamics and hybrid explicit-implicit solvation model for aqueous and nonaqueous solvents: GFP chromophore in water and methanol solution as case study. *J. Comput. Chem.* **2020**, *41*, 2228−2239.
(56) Petrone, A.; Lingerfelt, D. B.; Williams-Young, D. B.; Li, X. Ab Initio Transient Vibrational Spectral Analysis. *J. Phys. Chem. Lett.* **2016**, *7*, 4501−4508.
(57) Coppola, F.; Perrella, F.; Petrone, A.; Donati, G.; Rega, N. A Not Obvious Correlation Between the Structure of Green Fluorescent Protein Chromophore Pocket and Hydrogen Bond Dynamics: A Choreography From ab initio Molecular Dynamics. *Front. Mol. Biosci.* **2020**, *7*, 283.
(58) Hafner, J.; Wolverton, C.; Ceder, G. Toward Computational Materials Design: the Impact of Density Functional Theory on Materials Research. *MRS Bull.* **2006**, *31*, 659−668.
(59) Aarons, J.; Sarwar, M.; Thompsett, D.; Skylaris, C.-K. Perspective: Methods for Large-Scale Density Functional Calculations on Metallic Systems. *J. Chem. Phys.* **2016**, *145*, 220901.
(60) Beaulac, R.; Feng, Y.; May, J. W.; Badaeva, E.; Gamelin, D. R.; Li, X. Orbital Pathways for Mn^{2+}-Carrier *sp*−*d* Exchange in Diluted Magnetic Semiconductor Quantum Dots. *Phys. Rev. B* **2011**, *84*, 195324.
(61) Lestrange, P. J.; Nguyen, P. D.; Li, X. Calibration of Energy-Specific TDDFT for Modeling K-Edge XAS Spectra of Light Elements. *J. Chem. Theory Comput.* **2015**, *11*, 2994−2999.
(62) Petrone, A.; Goings, J. J.; Li, X. Quantum Confinement Effects on Optical Transitions in Nanodiamonds Containing Nitrogen Vacancies. *Phys. Rev. B* **2016**, *94*, 165402.
(63) Li, N.; Zhu, Z.; Chueh, C.-C.; Liu, H.; Peng, B.; Petrone, A.; Li, X.; Wang, L.; Jen, A. K.-Y. Mixed Cation $FA_xPEA_{1-x}PbI_3$ with Enhanced Phase and Ambient Stability toward High-Performance Perovskite Solar Cells. *Adv. Energy Mater.* **2017**, *7*, 1601307.

(64) Gary, D. C.; Flowers, S. E.; Kaminsky, W.; Petrone, A.; Li, X.; Cossairt, B. M. Single-Crystal and Electronic Structure of a 1.3 nm Indium Phosphide Nanocluster. *J. Am. Chem. Soc.* **2016**, *138*, 1510−1513.
(65) Donati, G.; Lingerfelt, D. B.; Aikens, C. M.; Li, X. Molecular Vibration Induced Plasmon Decay. *J. Phys. Chem. C* **2017**, *121*, 15368−15374.
(66) Xu, S.; Smith, J. E. T.; Gozem, S.; Krylov, A. I.; Weber, J. M. Electronic Spectra of tris-(2,2'-bipyridine)-M(II) Complex Ions in Vacuo (M = Fe and Os). *Inorg. Chem.* **2017**, *56*, 7029−7037.
(67) Raucci, U.; Chiariello, M. G.; Coppola, F.; Perrella, F.; Savarese, M.; Ciofini, I.; Rega, N. An electron density based analysis to establish the electronic adiabaticity of proton coupled electron transfer reactions. *J. Comput. Chem.* **2020**, *41*, 1835−1841.
(68) Petrone, A.; Perrella, F.; Coppola, F.; Crisci, L.; Donati, G.; Cimino, P.; Rega, N. Ultrafast photo-induced processes in complex environments: The role of accuracy in excited-state energy potentials and initial conditions. *Chem. Phys. Rev.* **2022**, *3*, 021307.
(69) Huix-Rotllant, M.; Ferré, N.; Barbatti, M. *Quantum Chemistry and Dynamics of Excited States*; John Wiley & Sons, Ltd, 2020; pp 13−46.
(70) Tavernelli, I.; Röhrig, U. F.; Rothlisberger, U. Molecular dynamics in electronically excited states using time-dependent density functional theory. *Mol. Phys.* **2005**, *103*, 963−981.
(71) Goings, J. J.; Kasper, J. M.; Egidi, F.; Sun, S.; Li, X. Real Time Propagation of the Exact Two Component Time-Dependent Density Functional Theory. *J. Chem. Phys.* **2016**, *145*, 104107.
(72) Lingerfelt, D. B.; Williams-Young, D. B.; Petrone, A.; Li, X. Direct Ab Initio (Meta-)Surface-Hopping Dynamics. *J. Chem. Theory Comput.* **2016**, *12*, 935−945.
(73) Petrone, A.; Williams-Young, D. B.; Lingerfelt, D. B.; Li, X. Ab Initio Excited State Transient Raman Analysis. *J. Phys. Chem. A* **2017**, *121*, 3958−3965.
(74) Horvath, R.; Fraser, M. G.; Clark, C. A.; Sun, X.-Z.; George, M. W.; Gordon, K. C. Nature of excited states of ruthenium-based solar cell dyes in solution: a comprehensive spectroscopic study. *Inorg. Chem.* **2015**, *54*, 11697−11708.
(75) Vlček, A., Jr; Záliš, S. Modeling of charge-transfer transitions and excited states in d^6 transition metal complexes by DFT techniques. *Coordin. Chem. Rev.* **2007**, *251*, 258−287.
(76) Monat, J. E.; Rodriguez, J. H.; McCusker, J. K. Ground-and Excited-State Electronic Structures of the Solar Cell Sensitizer Bis-(4,4'-dicarboxylato-2,2'-bipyridine)-bis-(isothiocyanato)ruthenium (II). *J. Phys. Chem. A* **2002**, *106*, 7399−7406.
(77) De Angelis, F.; Fantacci, S.; Selloni, A.; Nazeeruddin, M. K.; Grätzel, M. First-principles modeling of the adsorption geometry and electronic structure of Ru (II) dyes on extended TiO_2 substrates for dye-sensitized solar cell applications. *J. Phys. Chem. C* **2010**, *114*, 6054−6061.
(78) De Angelis, F.; Fantacci, S.; Mosconi, E.; Nazeeruddin, M. K.; Grätzel, M. Absorption spectra and excited state energy levels of the N719 dye on TiO_2 in dye-sensitized solar cell models. *J. Phys. Chem. C* **2011**, *115*, 8825−8831.
(79) Van Kuiken, B. E.; Huse, N.; Cho, H.; Strader, M. L.; Lynch, M. S.; Schoenlein, R. W.; Khalil, M. Probing the electronic structure of a photoexcited solar cell dye with transient x-ray absorption spectroscopy. *J. Phys. Chem. Lett.* **2012**, *3*, 1695−1700.
(80) Koposov, A. Y.; Cardolaccia, T.; Albert, V.; Badaeva, E.; Kilina, S.; Meyer, T. J.; Tretiak, S.; Sykora, M. Formation of assemblies comprising Ru−polypyridine complexes and CdSe nanocrystals studied by ATR-FTIR spectroscopy and DFT modeling. *Langmuir* **2011**, *27*, 8377−8383.
(81) Véry, T.; Ambrosek, D.; Otsuka, M.; Gourlaouen, C.; Assfeld, X.; Monari, A.; Daniel, C. Photophysical Properties of Ruthenium(II) Polypyridyl DNA Intercalators: Effects of the Molecular Surroundings Investigated by Theory. *Chem. Eur. J.* **2014**, *20*, 12901−12909.
(82) Daniel, C. In *Density-Functional Methods for Excited States*; Ferré, N., Filatov, M., Huix-Rotllant, M., Eds.; Springer International Publishing: Cham, 2016; pp 377−413.
(83) Ono, T.; Planas, N.; Miró, P.; Ertem, M. Z.; Escudero-Adán, E. C.; Benet-Buchholz, J.; Gagliardi, L.; Cramer, C. J.; Llobet, A. Carbon Dioxide Reduction Catalyzed by Dinuclear Ruthenium Polypyridyl Complexes. *ChemCatChem.* **2013**, *5*, 3897−3903.
(84) Planas, N.; Ono, T.; Vaquer, L.; Miró, P.; Benet-Buchholz, J.; Gagliardi, L.; Cramer, C. J.; Llobet, A. Carbon dioxide reduction by mononuclear ruthenium polypyridyl complexes. *Phys. Chem. Chem. Phys.* **2011**, *13*, 19480−19484.
(85) Heindl, M.; Hongyan, J.; Hua, S.-A.; Oelschlegel, M.; Meyer, F.; Schwarzer, D.; González, L. Excited-State Dynamics of $[Ru(S\text{-}Sbpy)(bpy)_2]^{2+}$ to Form Long-Lived Localized Triplet States. *Inorg. Chem.* **2021**, *60*, 1672−1682.
(86) Hua, S.-A.; Cattaneo, M.; Oelschlegel, M.; Heindl, M.; Schmid, L.; Dechert, S.; Wenger, O. S.; Siewert, I.; González, L.; Meyer, F. Electrochemical and Photophysical Properties of Ruthenium(II) Complexes Equipped with Sulfurated Bipyridine Ligands. *Inorg. Chem.* **2020**, *59*, 4972−4984.
(87) Jäger, M.; Freitag, L.; González, L. Using computational chemistry to design Ru photosensitizers with directional charge transfer. *Coordin. Chem. Rev.* **2015**, *304−305*, 146−165.
(88) Labat, F.; Ciofini, I.; Hratchian, H. P.; Frisch, M. J.; Raghavachari, K.; Adamo, C. Insights into Working Principles of Ruthenium Polypyridyl Dye-Sensitized Solar Cells from First Principles Modeling. *J. Phys. Chem. C* **2011**, *115*, 4297−4306.
(89) Ciofini, I.; Daul, C. A.; Adamo, C. Phototriggered Linkage Isomerization in Ruthenium-Dimethylsulfoxyde Complexes: Insights from Theory. *J. Phys. Chem. A* **2003**, *107*, 11182−11190.
(90) Ciofini, I.; Lainé, P. P.; Bedioui, F.; Adamo, C. Photoinduced Intramolecular Electron Transfer in Ruthenium and Osmium Polyads: Insights from Theory. *J. Am. Chem. Soc.* **2004**, *126*, 10763−10777.
(91) Lopata, K.; Van Kuiken, B. E.; Khalil, M.; Govind, N. Linear-Response and Real-Time Time-Dependent Density Functional Theory Studies of Core-Level Near-Edge X-Ray Absorption. *J. Chem. Theory Comput.* **2012**, *8*, 3284−3292.
(92) Tussupbayev, S.; Govind, N.; Lopata, K.; Cramer, C. J. Comparison of Real-Time and Linear-Response Time-Dependent Density Functional Theories for Molecular Chromophores Ranging from Sparse to High Densities of States. *J. Chem. Theory Comput.* **2015**, *11*, 1102−1109.
(93) Badaeva, E.; Albert, V. V.; Kilina, S.; Koposov, A.; Sykora, M.; Tretiak, S. Effect of deprotonation on absorption and emission spectra of Ru(II)-bpy complexes functionalized with carboxyl groups. *Phys. Chem. Chem. Phys.* **2010**, *12*, 8902−8913.
(94) Gunderson, V. L.; Krieg, E.; Vagnini, M. T.; Iron, M. A.; Rybtchinski, B.; Wasielewski, M. R. Photoinduced Singlet Charge Transfer in a Ruthenium(II) Perylene-3,4:9,10-bis(dicarboximide) Complex. *J. Phys. Chem. B* **2011**, *115*, 7533−7540.
(95) Campbell, L.; Mukamel, S. Simulation of x-ray absorption near edge spectra of electronically excited ruthenium tris-2,2'-bipyridine. *J. Chem. Phys.* **2004**, *121*, 12323−12333.
(96) Biasin, E.; Fox, Z. W.; Andersen, A.; Ledbetter, K.; Kjær, K. S.; Alonso-Mori, R.; Carlstad, J. M.; Chollet, M.; Gaynor, J. D.; Glownia, J. M.; Hong, K.; Kroll, T.; Lee, J. H.; Liekhus-Schmaltz, C.; Reinhard, M.; Sokaras, D.; Zhang, Y.; Doumy, G.; March, A. M.; Southworth, S. H.; Mukamel, S.; Gaffney, K. J.; Schoenlein, R. W.; Govind, N.; Cordones, A. A.; Khalil, M. Direct observation of coherent femtosecond solvent reorganization coupled to intramolecular electron transfer. *Nat. Chem.* **2021**, *13*, 343−349.
(97) Bianco, R.; Hay, P. J.; Hynes, J. T. Theoretical Study of O−O Single Bond Formation in the Oxidation of Water by the Ruthenium Blue Dimer. *J. Phys. Chem. A* **2011**, *115*, 8003−8016.
(98) Bianco, R.; Hay, P. J.; Hynes, J. T. Proton relay and electron flow in the O−O single bond formation in water oxidation by the ruthenium blue dimer. *Energy Environ. Sci.* **2012**, *5*, 7741−7746.
(99) Chong, E. Q.; Lingerfelt, D. B.; Petrone, A.; Li, X. Classical or Quantum? A Computational Study of Small Ion Diffusion in II-VI Semiconductor Quantum Dots. *J. Phys. Chem. C* **2016**, *120*, 19434−19441.

(100) Wong, M. W. Vibrational Frequency Prediction using Density Functional Theory. *Chem. Phys. Lett.* **1996**, *256*, 391−399.
(101) Barone, V.; Bloino, J.; Biczysko, M. Validation of the DFT/N07D computational model on the magnetic, vibrational and electronic properties of vinyl radical. *Phys. Chem. Chem. Phys.* **2010**, *12*, 1092−1101.
(102) Donati, G.; Lingerfelt, D. B.; Petrone, A.; Rega, N.; Li, X. Watching" Polaron Pair Formation from First-Principles Electron-Nuclear Dynamics. *J. Phys. Chem. A* **2016**, *120*, 7255−7261.
(103) Stein, J. L.; Steimle, M. I.; Terban, M. W.; Petrone, A.; Billinge, S. J. L.; Li, X.; Cossairt, B. M. Cation Exchange Induced Transformation of InP Magic-Sized Clusters. *Chem. Mater.* **2017**, *29*, 7984−7992.
(104) Gary, D. C.; Petrone, A.; Li, X.; Cossairt, B. M. Investigating the Role of Amine in InP Nanocrystal Syntheses: Destabilizing Cluster Intermediates by Z-Type Ligand Displacement. *Chem. Commun.* **2017**, *53*, 161−164.
(105) Chapman, C. T.; Liang, W.; Li, X. Ultrafast Coherent Electron-Hole Separation Dynamics in a Fullerene Derivative. *J. Phys. Chem. Lett.* **2011**, *2*, 1189−1192.
(106) Ding, F.; Chapman, C. T.; Liang, W.; Li, X. Mechanisms of Bridge-Mediated Electron Transfer: A TDDFT Electronic Dynamics Study. *J. Chem. Phys.* **2012**, *137*, 22A512.
(107) Petrone, A.; Lingerfelt, D. B.; Rega, N.; Li, X. From Charge-Transfer to a Charge-Separated State: A Perspective from the Real-Time TDDFT Excitonic Dynamics. *Phys. Chem. Chem. Phys.* **2014**, *16*, 24457−24465.
(108) Kasper, J. M.; Lestrange, P. J.; Stetina, T. F.; Li, X. Modeling $L_{2,3}$-Edge X-ray Absorption Spectroscopy with Real-Time Exact Two-Component Relativistic Time-Dependent Density Functional Theory. *J. Chem. Theory Comput.* **2018**, *14*, 1998−2006.
(109) Petrone, A.; Williams-Young, D. B.; Sun, S.; Stetina, T. F.; Li, X. An Efficient Implementation of Two-Component Relativistic Density Functional Theory with Torque-Free Auxiliary Variables. *Euro. Phys. J. B* **2018**, *91*, 169.
(110) Williams-Young, D. B.; Petrone, A.; Sun, S.; Stetina, T. F.; Lestrange, P.; Hoyer, C. E.; Nascimento, D. R.; Koulias, L.; Wildman, A.; Kasper, J.; Goings, J. J.; Ding, F.; DePrince, A. E., III; Valeev, E. F.; Li, X. The Chronus Quantum software package. *Wiley Interdiscip. Rev. Comput. Mol. Sci.* **2020**, *10*, No. e1436.
(111) Gaynor, J. D.; Petrone, A.; Li, X.; Khalil, M. Mapping Vibronic Couplings in a Solar Cell Dye with Polarization-Selective Two-Dimensional Electronic−Vibrational Spectroscopy. *J. Phys. Chem. Lett.* **2018**, *9*, 6289−6295.
(112) The dense electronic manifold and couplings among electronic states induce an ultrafast charge randomization among acceptor ligands of the initial localized excitation on very short time scales, thereby anticipating the competitive charge localization due to vibrations and potentially promoting an ultrafast charge injection into the substrate.
(113) Perrella, F.; Petrone, A.; Rega, N. Direct observation of the solvent organization and nuclear vibrations of $[Ru(dcbpy)_2(NCS)_2]^{4-}$, [dcbpy = (4,4'-dicarboxy-2,2'-bipyridine)], via ab initio molecular dynamics. *Phys. Chem. Chem. Phys.* **2021**, *23*, 22885−22896.
(114) Martin, R. L. Natural Transition Orbitals. *J. Chem. Phys.* **2003**, *118*, 4775−4777.
(115) Goings, J. J.; Lestrange, P. J.; Li, X. Real-Time Time-Dependent Electronic Structure Theory. *Wiley Interdiscip. Rev. Comput. Mol. Sci.* **2018**, *8*, No. e1341.
(116) Peng, B.; Lingerfelt, D. B.; Ding, F.; Aikens, C. M.; Li, X. Real-Time TDDFT Studies of Exciton Decay and Transfer in Silver Nanowire Arrays. *J. Phys. Chem. C* **2015**, *119*, 6421−6427.
(117) Donati, G.; Lingerfelt, D. B.; Aikens, C.; Li, X. Anisotropic Polarizability-Induced Plasmon Transfer. *J. Phys. Chem. C* **2018**, *122*, 10621−10626.
(118) The selection of the occupied and unoccupied molecular orbitals to be chosen for the "Koopman excitation" is based upon the electronic transition of interest between the singlet ground state (S_0) and the *n*th singlet excited state (S_n), whose main orbital contributions are resolved using preliminary frequency domain linear-response (hereafter LR)-TDDFT calculations. The choice of the experimentally relevant states of interest is guided by a comparison of spatial electronic density and electric dipole reorganization. These last quantities are computed via the preliminary LR-TDDFT features and allowed the association of the S_n states involved in the $S_0 \rightarrow S_n$ transitions with the ^{1}MLCT states, responsible for the ultrafast dynamics observed experimentally in the 2D electronic−vibrational spectra (ref 111 and Table S1 in the Supporting Information).
(119) Fischer, S. A.; Cramer, C. J.; Govind, N. Excited State Absorption from Real-Time Time-Dependent Density Functional Theory. *J. Chem. Theory Comput.* **2015**, *11*, 4294−4303.
(120) Bruner, A.; Hernandez, S.; Mauger, F.; Abanador, P. M.; LaMaster, D. J.; Gaarde, M. B.; Schafer, K. J.; Lopata, K. Attosecond Charge Migration with TDDFT: Accurate Dynamics from a Well-Defined Initial State. *J. Phys. Chem. Lett.* **2017**, *8*, 3991−3996.
(121) Bowman, D. N.; Asher, J. C.; Fischer, S. A.; Cramer, C. J.; Govind, N. Excited-state absorption in tetrapyridyl porphyrins: comparing real-time and quadratic-response time-dependent density functional theory. *Phys. Chem. Chem. Phys.* **2017**, *19*, 27452−27462.
(122) Benkö, G.; Kallioinen, J.; Korppi-Tommola, J. E.; Yartsev, A. P.; Sundström, V. Photoinduced ultrafast dye-to-semiconductor electron injection from nonthermalized and thermalized donor states. *J. Am. Chem. Soc.* **2002**, *124*, 489−493.
(123) Zobel, J. P.; González, L. The Quest to Simulate Excited-State Dynamics of Transition Metal Complexes. *JACS Au* **2021**, *1*, 1116−1140.
(124) Atkins, A. J.; González, L. Trajectory Surface-Hopping Dynamics Including Intersystem Crossing in $[Ru(bpy)_3]^{2+}$. *J. Phys. Chem. Lett.* **2017**, *8*, 3840−3845.
(125) Damrauer, N. H.; Cerullo, G.; Yeh, A.; Boussie, T. R.; Shank, C. V.; McCusker, J. K. Femtosecond dynamics of excited-state evolution in $[Ru(bpy)_3]^{2+}$. *Science* **1997**, *275*, 54−57.
(126) Kalyanasundaram, K. Photophysics, photochemistry and solar energy conversion with tris-(bipyridyl)ruthenium (II) and its analogues. *Coordin. Chem. Rev.* **1982**, *46*, 159−244.
(127) Juris, A.; Balzani, V.; Barigelletti, F.; Campagna, S.; Belser, P. l.; von Zelewsky, A. v. Ru (II) polypyridine complexes: photophysics, photochemistry, eletrochemistry, and chemiluminescence. *Coordin. Chem. Rev.* **1988**, *84*, 85−277.
(128) Kober, E. M.; Sullivan, B. P.; Meyer, T. J. Solvent dependence of metal-to-ligand charge-transfer transitions. Evidence for initial electron localization in MLCT excited states of 2,2'-bipyridine complexes of ruthenium (II) and osmium (II). *Inorg. Chem.* **1984**, *23*, 2098−2104.
(129) Dallinger, R. F.; Woodruff, W. H. Time-resolved resonance Raman study of the lowest (d π*, 3CT) excited state of tris-(2,2'-bipyridine)ruthenium (II). *J. Am. Chem. Soc.* **1979**, *101*, 4391−4393.
(130) Oh, D. H.; Boxer, S. G. Stark effect spectra of $Ru(diimine)_3^{2+}$ complexes. *J. Am. Chem. Soc.* **1989**, *111*, 1130−1131.
(131) Myrick, M.; Blakley, R.; DeArmond, M. Time-resolved photoselection of $[Ru(bpy)_3]^{2+}$-exciton hopping in the excited state. *J. Am. Chem. Soc.* **1987**, *109*, 2841−2842.
(132) Frisch, M. J.; Trucks, G. W.; Schlegel, H. B.; Scuseria, G. E.; Robb, M. A.; Cheeseman, J. R.; Scalmani, G.; Barone, V.; Petersson, G. A.; Nakatsuji, H.; Li, X.; Caricato, M.; Marenich, A. V.; Bloino, J.; Janesko, B. G.; Gomperts, R.; Mennucci, B.; Hratchian, H. P.; Ortiz, J. V.; Izmaylov, A. F.; Sonnenberg, J. L.; Williams-Young, D.; Ding, F.; Lipparini, F.; Egidi, F.; Goings, J.; Peng, B.; Petrone, A.; Henderson, T.; Ranasinghe, D.; Zakrzewski, V. G.; Gao, J.; Rega, N.; Zheng, G.; Liang, W.; Hada, M.; Ehara, M.; Toyota, K.; Fukuda, R.; Hasegawa, J.; Ishida, M.; Nakajima, T.; Honda, Y.; Kitao, O.; Nakai, H.; Vreven, T.; Throssell, K.; Montgomery, J. A., Jr.; Peralta, J. E.; Ogliaro, F.; Bearpark, M. J.; Heyd, J. J.; Brothers, E. N.; Kudin, K. N.; Staroverov, V. N.; Keith, T. A.; Kobayashi, R.; Normand, J.; Raghavachari, K.; Rendell, A. P.; Burant, J. C.; Iyengar, S. S.; Tomasi, J.; Cossi, M.; Millam, J. M.; Klene, M.; Adamo, C.; Cammi, R.; Ochterski, J. W.;

Martin, R. L.; Morokuma, K.; Farkas, O.; Foresman, J. B.; Fox, D. J. *Gaussian Development Version Revision J.02*, Gaussian, Inc.: Wallingford, CT, 2018.

(133) Becke, A. D. Density-Functional Thermochemistry. III. The Role of Exact Exchange. *J. Chem. Phys.* **1993**, *98*, 5648.

(134) Lee, C.; Yang, W.; Parr, R. G. Development of the Colle-Salvetti correlation-energy formula into a functional of the electron density. *Phys. Rev. B* **1988**, *37*, 785.

(135) Miehlich, B.; Savin, A.; Stoll, H.; Preuss, H. Results obtained with the correlation energy density functionals of Becke and Lee, Yang and Parr. *Chem. Phys. Lett.* **1989**, *157*, 200−206.

(136) Weigend, F.; Ahlrichs, R. Balanced basis sets of split valence, triple zeta valence and quadruple zeta valence quality for H to Rn: Design and assessment of accuracy. *Phys. Chem. Chem. Phys.* **2005**, *7*, 3297−3305.

(137) Andrae, D.; Haeussermann, U.; Dolg, M.; Stoll, H.; Preuss, H. Energy-adjusted ab initio pseudopotentials for the second and third row transition elements. *Theor. Chem. Acc.* **1990**, *77*, 123−141.

(138) Gaynor, J. D.; Petrone, A.; Li, X.; Khalil, M. Mapping Vibronic Couplings in Intramolecular Charge Transfer of a Solar Cell Dye with Polarization-Selective Two-Dimensional Electronic-Vibrational Spectroscopy. *J. Phys. Chem. Lett.* **2018**, *9*, 6289−6295.

(139) Li, X.; Smith, S. M.; Markevitch, A. N.; Romanov, D. A.; Levis, R. J.; Schlegel, H. B. A Time-Dependent Hartree-Fock Approach for Studying the Electronic Optical Response of Molecules in Intense Fields. *Phys. Chem. Chem. Phys.* **2005**, *7*, 233−239.

https://doi.org/10.1021/jacsau.2c00556
JACS Au 2023, 3, 70−79